Research in Astronomy and Astrophysics, 24:095018 (15pp), 2024 September https://doi.org/10.1088/1674-4527/ad7079

A Study of the Comets with Large Perihelion Distances C/2019 L3 (ATLAS) and C/2019 O3 (Palomar)

Alberto S. Betzler
Centro de Ciência e Tecnologia em Energia e Sustentabilidade, Universidade Federal do Recôncavo da Bahia, Feira de Santana, Bahia, 44.085-132, Brazil; betzler@ufrb.edu.br
Received 2024 June 9; revised 2024 August 3; accepted 2024 August 15; published 2024 September 18

Abstract

This work analyzes the photometric data of the Oort spike comets C/2019 L3 (ATLAS) and C/2019 O3 (Palomar) obtained between 2016 and 2023 by the ATLAS network and the Belgian Olmen Observatory. The comets Palomar and ATLAS have a typical and unusually high activity level, respectively, based on the Afρ parameter corrected to phase angle zero at perihelion. The absolute magnitude of comets ATLAS and Palomar in the o-band is 4.71 ± 0.05 and 4.16 ± 0.02 respectively. The cometary activity of comets ATLAS and Palomar probably began at $r > 13$ au before perihelion and will end at $r > 14$ au after perihelion, which means that they could remain active until the second half of 2026. The nucleus of comet ATLAS has a minimum radius of 7.9 km, and the nucleus of comet Palomar could be a little larger. The $c - o$ colors of the comets ATLAS and Palomar are redder and bluer, respectively, at perihelion than the solar twin YBP 1194. These comets showed a bluish trend in the coma color with decreasing heliocentric distance. Comet Palomar probably had two outbursts after its perihelion, each releasing about 10^8 kg of dust. The slopes of the photometric profile of the comae of these comets were between 1 and 1.5, indicating a steady state during the observation campaign.

Key words: comets: individual C/2019 L3 (ATLAS), C/2019 O3 (Palomar) – techniques: photometric – methods: data analysis

1. Introduction

Comets with large distances to perihelion ($q > 3$ au) (Marsden & Sekanina 1973), also known as long-period comets (LPCs), are minor bodies with orbital periods of centuries to many millennia, which can come from the other edge of the Oort cloud around 50,000 au (Weissman 1996). The study of these comets provides valuable information about the orbital dynamics and evolution of the solar system.

Gravitational interactions with giant planets and other external influences can alter their orbits in complex ways, leading to unpredictable orbital patterns and even close encounters with inner planets (Yabushita 1989; Natenzon et al. 1990; Wiegert & Tremaine 1999). The study of these orbital interactions not only allows us to better understand the dynamics of the solar system, but could also have significant implications for the assessment of the risks of impacts (Zimbelman 1984; Le Feuvre & Wieczorek 2008) and the long-term evolution of the solar system. This study is particularly affected by the fact that the comet observation campaigns miss a large number of LPCs making recurrent flybys in Saturn's region (near 10 au). The reason for this is that these comets fade away during previous, even more distant flybys outside Saturn and thus escape detection (Kaib 2022).

Therefore, analyzing their chemical composition can provide valuable insights into the original composition of the protoplanetary disk and the physico-chemical processes that took place during the early stages of planet formation (Eistrup et al. 2019; Willacy et al. 2022).

The detection of complex organic compounds such as amino acids and nucleotide precursors like glycine (Biver et al. 2014) or ethylene glycol and formamide (Hadraoui et al. 2019) in comets suggests that these objects may have served as carriers of essential organic molecules for the early Earth, directly influencing prebiotic chemistry and ultimately the emergence of life. The preservation of these substances in LPCs during their long journey from the Oort Cloud to the inner regions of the solar system provides a unique opportunity to study the fundamental components that contributed to the origin and evolution of life on Earth and possibly on other celestial bodies.

Despite their importance for the study of the formation and dynamic evolution of the solar system, LPCs with a large perihelion distance are poorly observed objects due to their low apparent brightness at perihelion. Their low brightness requires the use of large telescopes to improve the signal-to-noise ratio (SNR) for spectroscopic or photometric observations. These telescopes are highly sought-after instruments, so generally only a few nights per year are available for observing these comets. These limitations severely restrict our ability to understand them.

Comets C/2019 L3 (ATLAS) and C/2019 O3 (Palomar) were selected for the study to contribute to the investigation of long

perihelion distance LPCs. These objects are Oort spike comets (see Królikowska & Dybczyński 2017) with perihelion distances that are significantly different from each other ($q = 3.55$ and 8.82 au, respectively), so that the effects of solar distance on the cometary activity of these two objects can be compared.

Photometric data from the Asteroid Terrestrial-impact Last Alert System (ATLAS) network and the Olmen Observatory in Belgium were used for this study. Both comets were observed during the pre- and/or post-perihelion phases of their orbits with a median sampling rate of hours to weeks. The apparent magnitudes of the comets ATLAS and Palomar were measured with the broadband filters *o* and *c* in the ATLAS network and with a *G*-filter in the Olmen Observatory. This allowed the calculation of photometric parameters derived from the secular light curve in these three spectral bands, such as the absolute total magnitude, the activity indices, times, and heliocentric distances for the beginning and end of cometary activity (coma phase), the characterization of candidates for outbursts and an estimate of the diameters of the comet nuclei.

In the following, comets C/2019 L3 (ATLAS) and C/2019 O3 (Palomar) are referred to in the text as comets ATLAS and Palomar respectively.

2. The Data

The ATLAS and Palomar comets were observed by the ATLAS network. The four ATLAS twin telescopes with an aperture of 0.5 m were deployed at sites in the Northern Hemisphere (Haleakala and Mauna Loa, Hawaii, USA) and in the Southern Hemisphere (El Sauce, Chile and Sutherland, RSA) and detected potentially hazardous asteroids across the celestial sphere up to a magnitude of ∼19.7, in the orange ("*o*," wavelength range 560–820 nm) and cyan ("*c*," wavelength range 420–650 nm) bands (Tonry et al. 2018). The images of these two comets were taken with an exposure time of 30 s, in a sequence of four images over a period of about one hour (Smith et al. 2020). The apparent magnitudes were determined using the ATLAS Forced Photometry option, which performs a point-spread function (PSF) photometry of sources with celestial coordinates from the Jet Propulsion Laboratory's Horizons system.

The comets Palomar and ATLAS showed that their inner part of the coma exhibited a nearly stellar profile in both filters during the entire observation campaign (Figures 1 and 2), with near maximum apparent magnitudes of 16 and 8 at perihelion respectively. In this conjecture, the use of PSF photometry was particularly useful to correctly determine the apparent magnitude of two objects that crossed very densely populated star fields during the observing period of this study.

The apparent magnitudes *o* and *c* with errors of less than 0.1 mag for these two comets were considered for the analysis. This restriction led me to consider 1771 and 1175 magnitudes *o* and *c* for comets ATLAS and Palomar respectively. About 23% and 26% of the magnitudes of these comets were determined with the filter *c*. Comet ATLAS was observed between 2015 November 1 and 2024 February 18 UT and comet Palomar between 2017 August 16 and 2023 September 3 UT (Tables 1 and 2 respectively). These time spans also include observations prior to the discovery of the two objects (2019 June 10 for comet ATLAS and 2019 July 26 UT for comet Palomar).

The median sample rating for comet ATLAS and comet Palomar was around 0.2 hr for both filters.

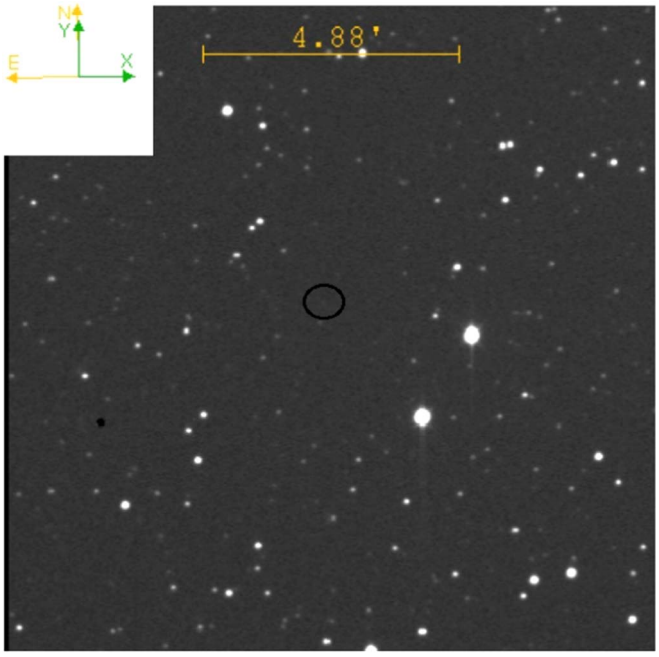

Figure 1. Image of comet ATLAS (oval) with filter *o*, taken in 2018 July, 24.208 UT by the ATLAS network. The field of view is $12\farcm3 \times 12\farcm3$ and the plate scale is $1\farcs85$ pixel^{-1}. The image was created with the software AstroImageJ in conjunction with the online application "astrometry.net."

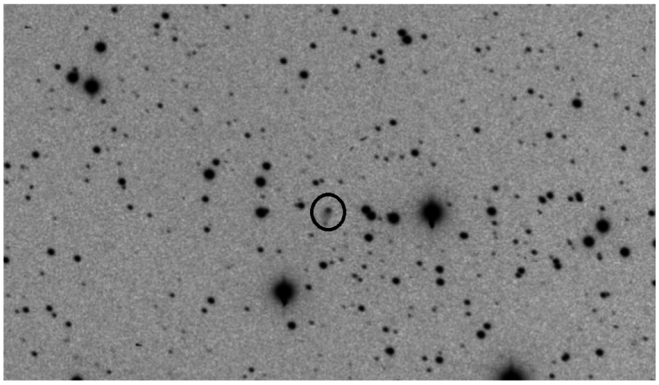

Figure 2. *G*-filter image of comet Palomar (oval), taken in 2021 September, 06.897 UT at the Olmen Observatory (Belgium). The field of view is $16\farcm2 \times 9\farcm37$ and the plate scale is $1\farcs38$ pixel^{-1}. The spatial orientation of this image is similar to that of Figure 1.

Table 1
Journal of Observations of Comet ATLAS

Filter	Start (UTC)	End (UTC)	N	α_{min}	α_{max}	r_{min}	r_{max}
G	2019-07-22.986	2022-11-18.221	47	2.634	15.950	3.555	8.187
o	2015-11-01.213	2024-02-18.021	1359	2.538	15.971	3.554	16.149
c	2016-06-11.021	2024-01-13.099	412	2.581	14.665	3.554	14.939

Note. The start and end of the observation campaign in each filter are in the format yyyy-mm-dd.ddd. N is the number of apparent magnitudes considered for the analysis. α_{min} (degree) and α_{max} (degree) are the minimum and maximum of the phase angles during each observation period. r_{min} (au) and r_{max} (au) are the corresponding heliocentric distances for these phase angles. These values do not necessarily correspond exactly to the time intervals "Start" and "End."

Table 2
Journal of Observations of Comet Palomar

Filter	Start (UTC)	End (UTC)	N	α_{min}	α_{max}	r_{min}	r_{max}
G	2021-07-18.030	2023-09-06.868	34	5.442	6.466	8.852	10.249
o	2017-08-26.383	2023-09-03.250	871	2.158	6.566	8.820	11.434
c	2017-08-16.393	2023-08-06.299	304	2.163	6.567	8.820	11.469

The magnitude error is approximately inversely proportional to the SNR (Howell 2000). The restriction of the maximum magnitude error imposed on the data of these two objects implies a minimum SNR of 10 for both objects. At these SNRs, the comets Palomar and ATLAS may be objects that are barely recognizable in an image. However, not all measurements have an apparent magnitude error that corresponds exactly to these error thresholds. The median of the errors is 0.02 and 0.05 mag for comets ATLAS and Palomar respectively, with a range of 0.001–0.1 mag for both objects considering the two filters.

The multi-aperture observations used for the analyzes in Sections 4.2, 4.3, 4.1 and 4.7 were taken by the Belgian amateur astronomer Alfons Diepens with a TEC 0.2 m f/9 refractor telescope equipped with an Optec NGUW 0.7XL focal reducer and an SBIG ST-10XME camera at the Olmen Observatory (MPC C23), a private observatory in Balen (Belgium). The data were taken through the G-band filter of an Astrodon RGB set. The centers and equivalent wavelength widths of the usual G-filter are 545 nm and 80 nm (Zhilyaev et al. 2021), respectively. These values almost correspond to the V-bands of the Johnson system with centers and equivalent widths of 550 nm with bandwidth of 80 nm (Moro & Munari 2000).

Comet Palomar was observed between 2021 July 18 and 2023 September 6 UT. The 34 apparent magnitudes[1] in the G-band were determined with a median sampling rate of 15 days.

Comet ATLAS was observed between 2019 July 22 and 2022 November 18 UT. A total of 47 measurements[2] were taken with a median sampling rate of eight days.

The apparent magnitudes were estimated with the Astrometrica[3] software in conjunction with the FoCAs[4] 2 in square aperture boxes with side lengths from 10″ to 60″ in regular steps of 10″. To analyze these data, an equivalent circular radius was defined that includes these boxes ($\rho = 7\farcs1$, $14\farcs1$, $21\farcs2$, $28\farcs3$, $35\farcs4$ and $42\farcs4$), since the inner coma of comets is approximately spherically symmetric. The photometric calibration of these magnitudes was performed with stars from the Gaia Data Release 2 (DR2) catalog.

3. Fitting the Secular Light Curve of Comets

The secular light curve of a comet can be interpreted as a combination of two components associated with the coma and the nucleus. If the comet is close to the Sun, e.g., at a distance of $r \leqslant 3$ au, the sublimation of volatiles, especially water, is probably the main source of cometary activity. At this phase, the luminous flux of the nucleus becomes negligible compared to the contribution of the coma for most comets. However, as the comet moves farther away from the Sun and approaches distances where cometary activity decreases, the nucleus becomes the dominant factor in the secular curve. Therefore, accurately determining the apparent magnitude of a comet with and without a coma is crucial to understanding its behavior at different distances from the Sun.

The apparent magnitude m of a comet with a coma $m(\Delta, r)$ is given by

$$m(\Delta, r) = m(1, 1) + 5\log_{10}\Delta + 2.5n\log_{10} r, \qquad (1)$$

[1] https://www.astronomie.be/alfons.diepvens/cometimages/comet/photometry/C2019-O3-Palomar.html
[2] https://www.astronomie.be/alfons.diepvens/cometimages/comet/photometry/C2019-L3-ATLAS.html
[3] http://www.astrometrica.at/
[4] http://www.astrosurf.com/orodeno/focas/

where r and Δ are the heliocentric and geocentric distances of the comet respectively, $m(1,1)$ is the absolute magnitude of the comet at Δ and r equals 1 au.

The magnitude M of a low activity or inactive comet nucleus at different phase angles α is given by

$$M(\Delta, r, \alpha) = M(1, 1, 0) + 5\log_{10}\Delta r + \beta\alpha, \quad (2)$$

where β is the phase coefficient (degree^{-1}) and $M(1,1,0)$ is the nuclear absolute magnitude.

4. Results and Analyses

In this paper, the parameters derived from the data are divided into activity and photometric parameters. Activity parameters are closely related to the activity of the comet and are the time and solar distance for the activation and deactivation of the nucleus, the activity index n (Equation (1)) and the Afρ parameter at perihelion, corrected to zero phase. Photometric parameters are the absolute magnitude of the comet $m(1,1)$ (Equation (1)), the absolute nuclear magnitude $M(1,1,0)$ (Equation (2)), and the absolute color Δm and relative activity indices Δn as well as the nuclear phase coefficient β.

The Afρ parameter at perihelion corrected to a phase angle of zero degrees is defined in Section 4.1.

The time and solar distance for the activation and deactivation of the nucleus and the nuclear phase coefficient β are defined in Section 4.3.

The absolute color Δm and the relative activity indices Δn are defined in Section 4.4.

The data were separated by filter and the time span relative to perihelion to determine the photometric and activity parameters of comets ATLAS and Palomar with and presumably without coma (nucleus).

Possible outliers were excluded from the following analysis before optimization with Tukey's fence method (Tukey et al. 1977) with a standard number of samples $k = 1.5$. The nature of these outliers is examined in Section 4.6.

4.1. The Afρ Parameter and Activity Level

The Afρ parameter, a proxy for the dust emission rate, was defined by A'Hearn et al. (1984) and can be expressed as follows

$$\mathrm{Af}\rho = 4\,\frac{r^2\Delta^2}{\rho}\,10^{0.4(m_\odot - m(r,\Delta))}, \quad (3)$$

where $m_\odot$ is the photovisual solar apparent magnitude (-26.73 ± 0.03, Stebbins & Kron 1957). A is the dust Bond albedo at the phase angle considered, and f is the filling factor.

The absolute magnitude of the Sun is 4.85 using -26.73 ± 0.03 as the apparent magnitude of the Sun, which in the Vegamag system is close to the value of 4.81 proposed by Willmer (2018).

The apparent magnitude $m(\Delta, r)$ for active comets shows a dependence on the aperture radius ρ, which is adjusted by Betzler et al. (2017) as follows

$$m(\Delta, r) = 2.5(s - 2)\log_{10}(\rho) + c_0, \quad (4)$$

where s is the exponent of the relationship between the photometric flux F and ρ of type $\mathrm{F} \sim \rho^{-s}$, assuming that the coma has a radial outflow, and c_0 is the optocentric magnitude.

The parameter Afρ (cm) depends on the phase angle α. The correction of the influence of the phase angle was made using the relationship

$$\mathrm{Af}\rho(0) = \frac{\mathrm{Af}\rho}{\phi(\alpha)}, \quad (5)$$

$\phi(\alpha)$ is the Schleicher dust phase function.[5]

The $\phi(\alpha)$ function used in this paper is the polynomial fit of the Schleicher curve as proposed by Blaauw et al. (2014).

Equations (2) and (5) use different phase relationships. The first equation uses a classic linear phase function that approximately describes the Schleicher curve for phase angles below 30°. Equation (5) was used to describe the apparent magnitude of a comet with low activity, where a significant part of the luminous flux presumably comes from the reflection of sunlight on the surface of the nucleus. Since the comet is far from the Sun, the phase angle is always less than 30°. This equation was used in conjunction with Equation (1) to determine the heliocentric distance corresponding to the beginning and end of the comet's activity in Section 4.3.

The dependence between the Afρ parameter and the photometric aperture ρ can be adjusted by combining Equations (3) and (4). Figures 3 and 4 show that this dependence tends to a horizontal asymptote value of the parameter Afρ. It has already been shown that the parameter Afρ varies with the size of the photometric aperture in almost all cases. Theoretically it should not, but it does. This is the main reason why this parameter should be treated with great caution and not overinterpreted or overanalyzed.

A common method in comet photometry is to link the aperture radius ρ (in arcseconds) with a constant optocentric distance in kilometers (e.g., 10,000 km). Betzler et al. (2018, 2020) and Betzler & de Sousa (2020) have shown that the application of this method causes systematic errors in the magnitudes of comets 1P/Halley, 4P/Faye, 63P/Wild, C/2012 K1 (PANSTARRS) and C/2014 S2 (PANSTARRS). This systematic error can obviously be transferred to the Afρ parameter.

In our Belgian data set, the angular diameter of the coma during the observing season of these two comets was probably small compared to the aperture radius of 42.″4, causing the observed trend. This hypothesis is supported by the data, as about 90% of the luminous flux measured at 42.″4 is also measured at 28.″3, as shown by the observation of comet

[5] https://asteroid.lowell.edu/comet/dustphase.html

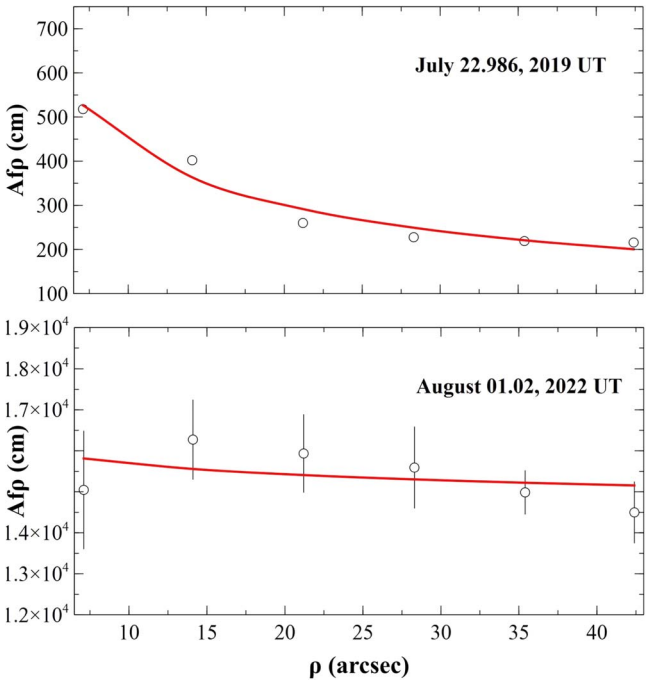

Figure 3. Relationship between the Afρ parameter and the photometric aperture radius ρ for comet ATLAS at different observation times before (top, $r = 8.187$ au and $\alpha = 6.^{\circ}895$) and after perihelion (bottom, $r = 3.554$ au and $\alpha = 2.^{\circ}634$). The solid red line represents a model to describe the last relationship, which results from the combination of Equations (3) and (4).

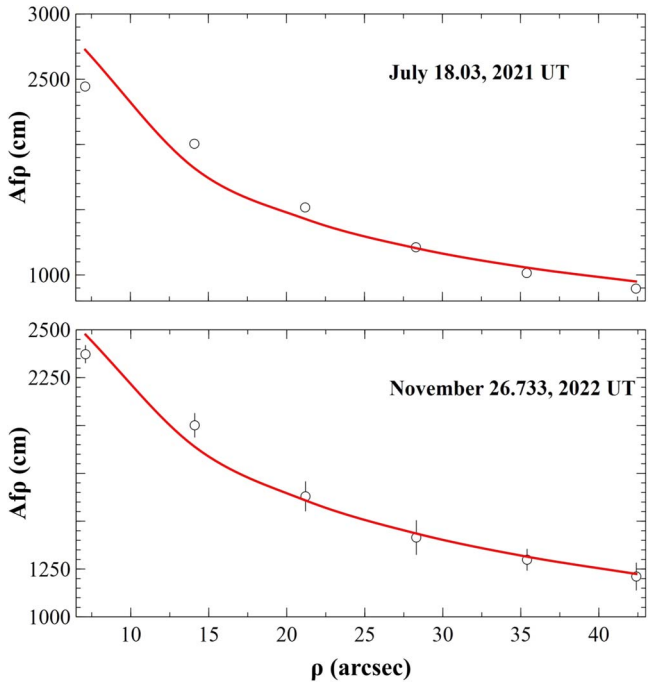

Figure 4. Relationship between the Afρ parameter and the photometric aperture radius ρ for comet Palomar at different observation times before perihelion. Top: $r = 8.852$ au and $\alpha = 6.322$ degrees. Bottom: $r = 9.533$ au and $\alpha = 5.^{\circ}920$.

Palomar on 2021 July 18. A similar trend was observed for comet C/2012 J1 (Catalina) by Betzler & de Sousa (2023).

The angular diameter of the coma of these two comets was probably small compared to the aperture radius of $42.''4$. Therefore, the apparent magnitudes measured with this aperture radius were used to calculate the parameter Afρ.

The use of an aperture radius of $42.''4$ makes it possible to classify the activity level of comets ATLAS and Palomar according to the scheme defined by Betzler et al. (2023), which uses the same aperture radius. The activity level of comets ATLAS and Palomar was classified by investigating the dependence of the parameter Af$\rho(0)$ on the heliocentric distance r.

The relationship Af$\rho(0) \times r$ was empirically adjusted with a double exponential function proposed by Ehlert et al. (2019).

$$\mathrm{Af}\rho(x) = \begin{cases} K_1 + \mathrm{Af}\rho(x_{\max}) * 10^{-\gamma_1 |x - x_{x_{\max}}|} & x \leqslant 0 \\ K_1 + \mathrm{Af}\rho(x_{\max}) * 10^{-\gamma_2 |x - x_{x_{\max}}|} & x \geqslant 0 \end{cases}, \quad (6)$$

where K_1 is the asymptotic value of Afρ and γ_1 and γ_2 correspond to the logarithmic slopes of the ascending and descending parts of the function relative to its maximum Af $\rho(x_{\max})$ respectively.

x is the normalized heliocentric distance, defined as

$$x = (r - q)\frac{t - t(q)}{|t - t(q)|}, \quad (7)$$

where q and $t(q)$ are the perihelion distance and the time of perihelion, respectively.

The relationship between the G-band Af$\rho(0)$ of comets ATLAS and Palomar and x was fitted in Equation (6) (Figure 5). The fit shows that the coefficients γ_1 and γ_2 have no obvious correlation with the photometrically derived activity index for both comets. The Af$\rho(0) \times x$-curve of comet ATLAS is strongly asymmetric, and its $\gamma_1 > \gamma_2$ reflects a slow decrease in dust emission with the increase in heliocentric distance. This post-perihelion trend is also observed for comet Palomar.

The values of Af$\rho(0)(x_m = 0)$ at perihelion are $26{,}044 \pm 171$ cm for comet ATLAS and 2069 ± 163 cm for comet Palomar. These values can be used to classify the activity level according to the scheme proposed by Betzler et al. (2023). However, this scheme is based on the value Af$\rho(0)(x_m = 0)$ measured by the filter R. Is a comparison with the Af$\rho(0)(x_m = 0)$ measured in the G-band possible? The difference between the Afρ measured with the same photometry aperture and filters R and V for three comets of different types estimated by Mazzotta Epifani et al. (2010), Picazzio et al. (2019) and Shi et al. (2023) is always smaller than 20%, which can be considered small for comparison purposes due to the wider range of activity classes.

Comet ATLAS is one of the unusual comets with high activity. C/2014 Q2 (Lovejoy) also belongs to the unusual class as it is the

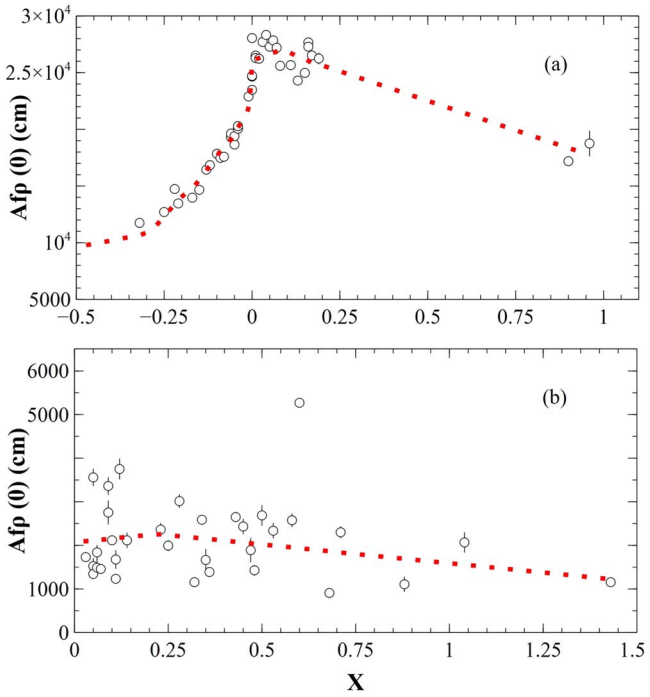

Figure 5. Relationship between the parameter Afρ(0) and the normalized heliocentric distance x for comet ATLAS (a) and Palomar (b). The red dots in panel (a) represent the fit of Equation (6) to the observed relationship, with k1 = 2046.10 cm, Af$\rho(x_{max}) = 25016.4$ cm, $x_{max} = 0.082$ $\gamma_1 = 1.14$, and $\gamma_2 = 0.22$. The fit of Equation (6) to the observed relationship corresponds to the red dots in panel (b), with k1 = −24754.99 cm, Af$\rho(x_{max}) = 27018.94$ cm, $x_{max} = 0.22$ and $\gamma_2 = 0.014$. All parameters have two decimal places by convention. The peak of the Afρ(0) parameter after perihelion ($x = 0$) for comet Palomar can be explained by an increased activity of the comet, but cannot be identified as an outburst using Tukey's fence method.

most active LPC in the entire sample analyzed by Betzler et al. (2023), but comet ATLAS is even more active. Jehin et al. (2022) estimated a dust/gas ratio $\log[A(0)f\rho(BC)/Q(CN)] = -21.71$ only 12 days after perihelion, indicating that this comet is very dusty compared to the ratio of -23.3 ± -0.3 proposed by A'Hearn et al. (1995) for typical comets.

Comet Palomar has a typical level of activity. "Typical" comets in terms of activity level like comet Palomar are more frequent between short periods than LPCs and with percentages of 72.7% and 53.6%, respectively.

4.2. *Absolute Magnitude* m*(1,1) and Activity Indices* n

The determination of the absolute magnitude $m(1,1)$ and the activity indices n_1 before and n_2 after perihelion can easily be achieved by unconstrained nonlinear optimization using the generalized reduced gradient method with appropriate initial values (Figures 6 and 7). The input values for these constants were derived empirically from a superposition between the model defined by Equation (1) and the observational data.

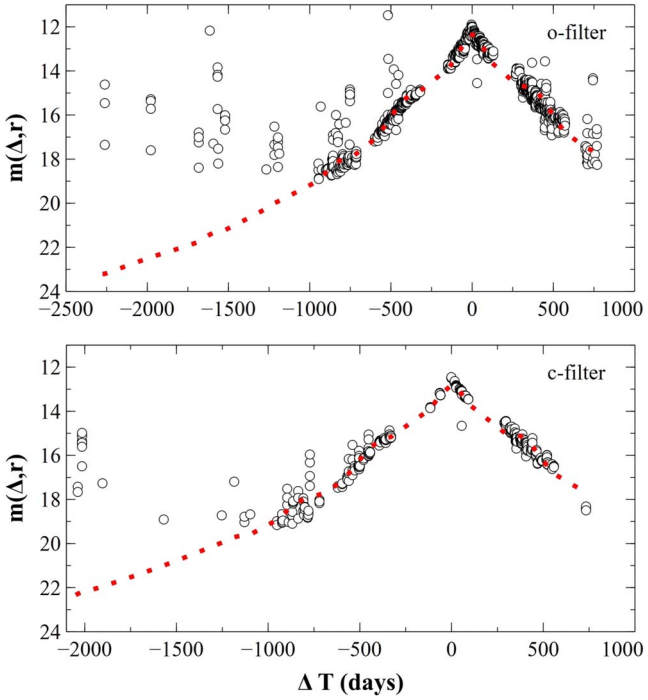

Figure 6. o- and c-filter secular light curves of comet ATLAS. ΔT is the measurement in days until perihelion passage. The red dotted lines correspond to the best fit of Equation (1) to the observed secular curve. Outliers identified using the Tukey's fence method were excluded from this fit.

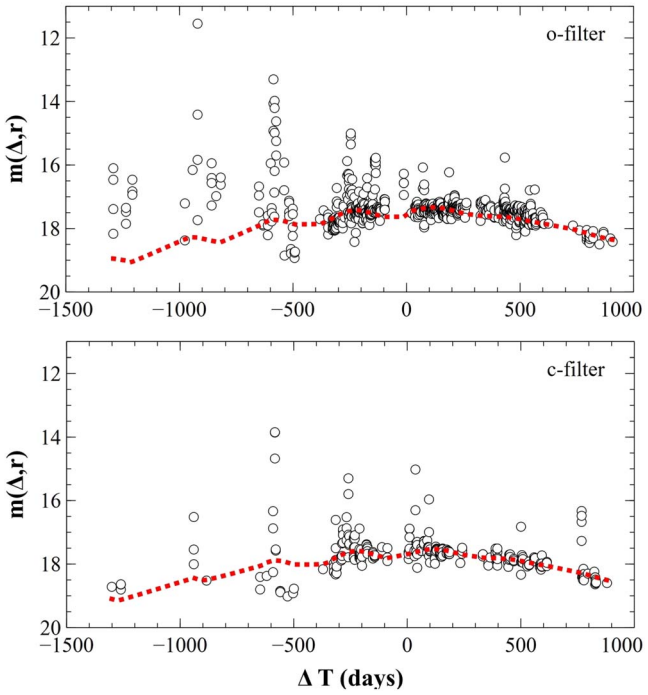

Figure 7. o- and c-filter secular light curves of comet Palomar. Outliers identified using Tukey's fence method were excluded from this fit.

Table 3
Photometric Parameters of Comet ATLAS

Filter	$m(1,1)$	n_1	n_2
G	5.1 ± 0.4	2.8 ± 0.4	2.5 ± 0.4
o	4.71 ± 0.05	4.13 ± 0.03	4.06 ± 0.03
c	5.74 ± 0.07	3.65 ± 0.05	3.63 ± 0.05

Note. $m(1, 1)$ is the absolute magnitude. n_1 and n_2 are the activity indices before and after perihelion respectively.

Table 4
Photometric Parameters of Comet Palomar

Filter	$m(1,1)$	n_1	n_2
G	5.5 ± 0.6	x	0.6 ± 0.2
o	4.16 ± 0.02	3.7	3.6
c	4 ± 1	3.7 ± 0.4	3.7 ± 0.4

Note. The calculated error of the o-filter activity indices is less than 0.001. It was decided to represent these parameters with two significant figures.

The ideal value for these parameters resulting from the optimization is the one that minimizes the objective function χ^2.

The absolute magnitudes and activity indices for the comets ATLAS and Palomar are given in Tables 3 and 4. The $m(1,1)$ magnitudes and the indices n in the o-filter for comet ATLAS are systematically brighter and greater, respectively, than the values estimated with the c-filter. On the other hand, both parameters are similar for comet Palomar. This tendency is probably related to the color of the cometary dust that makes up the bulk of the spectra of these comets, as well as to the possible but unverified presence of emission lines from CN, C_3, C_2, and NH_2 gas species (Meech & Svoren 2004), especially in the c-band.

The activity indices n before and after perihelion of these two comets in the o- and c-filter are equal if their error bars are taken into account. This means that the secular light curve is symmetric relative to perihelion, which is quite common for short- and long-period comets (Betzler et al. 2023) and might reflect the continuous activity of the same region on the nuclei (Hughes 1989; Moulane et al. 2023).

The absolute magnitude in the G filter calibrated with the Gaia catalog lies between the $m(1,1)$ magnitudes estimated with the o and c filters for comet ATLAS and is systematically less bright for these two filters for comet Palomar (Tables 3 and 4 and Figure 8). The activity indices n for both comets are systematically lower than these parameters estimated with the o and c filters. The differences between the absolute magnitudes in the c- and G-filter are probably not related to the color of the coma. Presumably, the absolute magnitudes in the c and G filters could be similar due to their similar spectral range. All

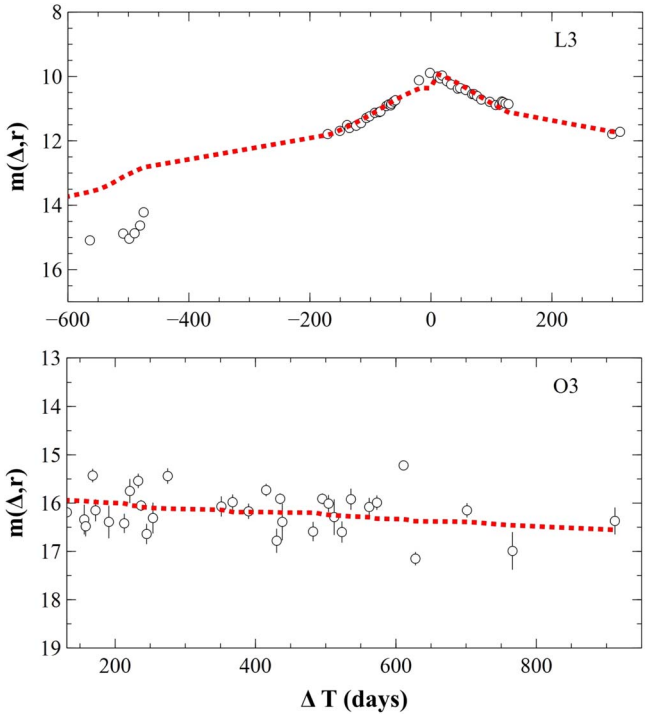

Figure 8. G-filter secular light curves of comet ATLAS (L3) and Palomar (O3).

these differences can be explained by the time span before or/and after perihelion, which is almost three times larger in the ATLAS data than in the Belgian data. Hump-shaped patterns are common in the secular light curve of a comet (Ferrín 2010) and are caused by fluctuations in the comet's activity, such as prolonged outbursts or nuclear splitting, which can cause a decrease or increase in the n-index and absolute magnitude values.

For comets ATLAS and Palomar, there were some candidates for outbursts during the observation campaign corresponding to the Belgian data. The nature of these events is investigated in Section 4.6.

4.3. Beginning and End of Comet Activity

The beginning and end of the comet's activity can be easily determined if one assumes that there is a heliocentric distance at which the apparent magnitudes described by Equations (1) and (2) are equal. The determination of this distance r is a simple optimization task if all parameters of these two equations are known, but unfortunately this is not the case for the nuclear absolute magnitude $M(1,1)$ and the phase coefficient β in Equation (2). These parameters can be estimated based on comet population statistics or photometric data collected when the comet is far from the Sun.

The study of comet nuclei observed at large distances from the Sun suggests that $\beta = 0.05$ degrees^{-1} (Knight et al. 2023) is

a reasonable value for this constant, although it is obtained for short period comets (SPCs).

The apparent magnitude measurements of comets ATLAS and Palomar made more than 1000 days before perihelion are not visually consistent with the trend of most data. In a first approach, these magnitudes could be associated with an inactive or extremely weakly active cometary nucleus and estimated for the $M(1,1,0)$ magnitude of Equation (2) by optimization as applied to the estimation of the parameters in Equation (1). However, less than a dozen measured values are available for each comet.

As an alternative, the optocentric magnitude c_0 of Equation (4) was used to define the absolute magnitude of the nuclei. The magnitude c_0 was estimated by fitting this last equation to the relationship between the apparent magnitude m (Δ, r) measured at different photometric apertures.

The optocentric magnitudes were estimated from observations in which these comets were as far away from the Sun as possible in order to obtain values close to the apparent nuclear magnitudes.

The data on comet ATLAS were recorded on 2019 July 22.9865 UT, when the object was 8.19 and 7.87 au away from the Sun and Earth, respectively. The comet was still 901.7 days away from reaching perihelion. The corresponding phase angle was $6^{\circ}.90$. Applying Equation (4) to the multiaperture data yields $c_0 = 19.6 \pm 0.4$. The candidate for the absolute nuclear magnitude $M(1,1,0)$ is then 10.2 ± 0.4 using Equation (2).

The data on comet Palomar were obtained on 2023 September 6.8681 UT, when the object was 10.25 and 10.47 au from the Sun and Earth, respectively. The comet was observed 911.3 days before perihelion. The corresponding phase angle was $5^{\circ}.44$. Applying Equation (4) to the data yields $c_0 = 19.3 \pm 0.1$. The candidate for the absolute nuclear magnitude $M(1,1,0)$ is 8.9 ± 0.1.

With these initial values of the nuclear magnitudes of the comets ATLAS and Palomar, two doubts may arise: (a) Were the comets active at the observation times considered? (b) How large is the difference between the magnitude estimated with the G-filter and calibrated with the Gaia catalog and the values obtained with the o- and c-filters?

Both comets were probably active at the analyzed observation times. This can be deduced from the $Af\rho(0)$ parameters of these objects at the observation times: 428 ± 22 cm for comet ATLAS and 1155 ± 37 cm for comet Palomar, both measured with a photometric box of $60''$ side. These values are considerably high and compatible with the $Af\rho(0)(x_m = 0)$ for typical and moderately active short-period comets (Betzler et al. 2023), but they are smaller when compared to the activity peak of these comets. It is quite plausible that the start and end of cometary activity for the comets ATLAS and Palomar occur at greater solar distances than the calculated distances r.

Question (b) can be answered by analyzing the difference between the magnitudes of an object measured with the o and c filters of the ATLAS network and other photometric systems with broadband filters near the G-band. The selected object for the analysis is the star Cl* NGC 2682 YBP 1194 and the photometric system is the Johnson-Cousins system. This star is a solar twin in the open star cluster M67 (Liu et al. 2016) and was chosen because it serves as a reference for the solar colors for further analyses in this manuscript. This star has a mean o- and c-magnitude of 14.37 ± 0.02 (1σ) and 14.641 ± 0.007 respectively, based on 69 and 19 measurements since 2024 January 29 UT. The corresponding magnitudes $B = 14.6 \pm 0.1$ and $V = 15.3 \pm 0.2$ are from AAVSO Photometric All-Sky Survey (APASS) Data Release 10 (Henden 2019). The o- and c-filters of the ATLAS network were developed to enable the detection of asteroids that are roughly differentiated by their albedo. Due to this property, their bandpasses have a significant intersection, which justifies the low value of the $c - o$ color index 0.27 ± 0.03 compared to $B - V = 0.7 \pm 0.3$. The absolute value of this $B - V$ color is compatible with the solar value (0.64 ± 0.02 from (Holmberg et al. 2006)) despite the large error.

If we compare the V magnitude of YBP 1194 with its o and c magnitudes, we find a difference of 0.24 and -0.034 mag respectively. The difference with respect to the B filter is greater with corresponding values of 0.91 and 0.64 mag.

Due to the smaller difference between the G-band magnitude and the c magnitudes, the heliocentric distance for the beginning and end of the comet activity was estimated based on the c-band data for both comets.

It is interesting that, according to the optimization, the beginning of comet activity of comet ATLAS and Palomar was at $r > 13$ au before perihelion and its end at $r > 14$ au after perihelion, which means that the two comets will possibly still be active until the second half of 2026.

The sustainability of the activity of comets at such large distances is still debated in the literature (Kelley et al. 2022). The activity of comets ATLAS and Palomar could be driven by the sublimation of low sublimation temperature materials such as carbon monoxide or dioxide and/or exotic cometary volatiles such as ammonia, formaldehyde or methane (Delsemme 1982; Meech & Svoren 2004). The carbon monoxide or dioxide ices are promising candidates for the source of cometary activity, as they are more abundant in the comet population (A'Hearn et al. 2012; Harrington Pinto et al. 2022) and the other substances contribute little, at most a few percent, to the coma gas or are hardly detectable in remote observations of comets (Krankowsky 1991; Faggi et al. 2019).

The sublimation temperature of carbon monoxide and carbon dioxide ice is 25 and 72 K (Womack et al. 2017) respectively, which may mean that the sublimation of carbon monoxide can take up to several tens of astronomical units, since the temperature of a blackbody sphere at 14 au $\sim$ is 70 K.

Phase transitions of water ice can also drive cometary activity of comets, but their role as a major player in the

activity of comets ATLAS and Palomar is questionable because the low nuclei temperatures at 14 au are too low to either sublimate water ice or crystallize amorphous ice (Jewitt et al. 2017). But even this conclusion should be taken with caution, because it is still controversial whether the crystallization process is exothermic or endothermic, and that the depth at which amorphous ice can survive depends essentially on the latent heat of ice crystallization (Arakawa & Wakita 2024).

4.4. Absolute Colors and Relative Activity Indices

Spectrophotometric observations of comets are usually carried out with narrow-band filters to isolate more relevant emission lines such as those of CN, C_2 or C_3 (Vanysek 1983). This type of observation led to a first taxonomy of comets based on their chemical content (A'Hearn et al. 1995). Some broadband filters in the long wavelength range, e.g., in the near-infrared, such as the International Halley Watch or the Hale-Bopp sets, are used to estimate the dust emission rate and calculate its ratio to the gas components of the coma. If a comet is far from the Sun and shows no activity, its nucleus can be taxonomically classified according to an asteroid scheme based on its Johnson-Cousins *BVRI* colors.

Ayala-Loera et al. (2018) defined the absolute color and relative phase coefficients in two broadband colors to investigate the surface properties of transneptunian objects (TNOs). A negative correlation was found between the absolute color and the relative phase coefficients for an analyzed population of these objects. This correlation is probably related to the effect of phase reddening on the surface of these objects. For comets, the same absolute color can be defined based on the difference between the absolute magnitudes $m(1,1)$ derived from the secular curve in the o- and c-band. The relative activity index Δn can be defined by the difference between the activity indices determined with c- and o-filters before and after perihelion. In contrast to TNOs, this relative activity index measures the gradient of the change in coma color with heliocentric distance, i.e., the comet became red near the Sun and blue far from the Sun. Jewitt & Meech (1988), Solontoi et al. (2012), Jewitt (2015) and Betzler et al. (2017) have come to the conclusion that there is no correlation between the visible and infrared colors of comets and the heliocentric distance. This idea implies that Δn is zero and obviously contradicts the trend between color and heliocentric distance found in loco on comet 67P/Churyumov-Gerasimenko by Filacchione et al. (2020).

The absolute colors and relative activity indices of comets ATLAS and Palomar are listed in Table 5. The differential index makes it easy to determine whether the color of the comet has a bluish or reddish tendency or not, depending on whether this parameter is negative, positive or zero near the Sun. The absolute color is the color index of the comet at heliocentric and geocentric distances of 1 au and provides a standardized reference for comparing comet and solar colors.

Table 5
$c-o$ Absolute Colors $\Delta m(1,1)$ and Relative Activity Indices Δn of Comets ATLAS and Palomar

Comet	$\Delta m(1,1)$	Δn_1	Δn_2
L3	1.0 ± 0.1	-0.48 ± 0.08	-0.43 ± 0.08
O3	0 ± 1	0.0 ± 0.4	0.1 ± 0.4

Note. Δn_1 and Δn_2 are the relative activity indices before and after perihelion, respectively.

There is a clear color-distance trend for comet ATLAS, where the comet's color became bluer near the Sun after and before perihelion passage. For comet Palomar, this color trend is very questionable as the relative activity indices are nearly zero and have a large error.

The absolute colors of comet ATLAS are redder than the $c-o$ color of the star YBP 1194, the solar twin that serves as a reference in this manuscript. On the other hand, the $\Delta m(1,1)$ color of comet Palomar is lower than the solar color despite its large error bar. The comet ATLAS is redder at perihelion than the centaur 29P/Schwassmann–Wachmann with an absolute color of 0.2 ± 0.2 and the dwarf planets Pluto and Eris (Betzler 2024). The zero color of comet Palomar is not unrealistic if one considers the lower limit of the absolute color of centaur 29P, which is defined by its error.

The absolute red color of comet ATLAS determined in this study is consistent with the mean $B-V$ color index of 0.8 ± 0.1 (1σ) based on 12 measurements of Sun et al. (2024) taken with a nearly constant photometric aperture of $22''$ between 2021 March 28.729 and May 14.721 UT prior to perihelion passage on 2022 January 09.711 UT. Despite the small sample size, the $B-V$ color distribution can be adjusted by a Gaussian distribution determined by the Shapiro–Wilk test (p-value[6] $= 0.3096$), which is greater than the significance level $\alpha = 0.05$. This means that the 68% of $B-V$ colors during the 36 days of their observation campaign are between 0.7 and 0.9, which is consistent with the temporal order of variation of weeks for *BVRI* colors of the activity of comets defined by Betzler et al. (2017). The runs test does not indicate that this variation is random (p-value < 0.05), which supports the idea that these variations in $B-V$ color may be related to the rotation period of the nucleus (Leibowitz & Brosch 1986a, 1986b; Betzler & de Sousa 2020). The short-term variations in the $B-V$ color of comet ATLAS are related to the nuclear activity of this object and not to the change in shape or albedo spots on the nucleus. Figure 2 of Sun et al. (2024) shows that comet ATLAS had an expressive coma during the observation period considered in this study.

[6] Dahiru (2008) provides an explanation of the meaning of the p-value.

A similar variation of the $o-c$ color index with heliocentric distance is observed for both comets, but with different extent, as suggested by the values of the different activity indices Δn.

The ATLAS telescopes did not observe the comets with a time interval of a few seconds or minutes between successive images with the o- and c-filters, but days or several dozen days. This peculiarity leads to $c-o$ colors with values far from the color index of the solar twin YBP 1194, but a direct comparison between them can help to deduce the dependence of the $c-o$ color index on the heliocentric distance r. These $o-c$ color indices were divided into groups of four $c-o$ color measurements for comet ATLAS and Palomar in the pre-perihelion phase. The median value of the $c-o$ color of comet ATLAS for $14.81 < r < 9.97$ au is 0.62 and for $8.3 < r < 8.1$ au is 0.40. The median value of the $c-o$ color of comet Palomar for $11.67 < r < 10.32$ au is 1.275 and for $9.57 < r < 9.45$ au is 0.70. These results indicate that the median color indices of both comets become blue with decreasing heliocentric distance, as suggested by their relative activity indices, despite the large error these indices have for comet Palomar.

The scatter of the $c-o$ color indices of these two comets between the considered heliocentric distance ranges was between 0.2 and 0.7 mag. The scatter increases as the heliocentric distance decreases, suggesting a correlation with the increase in cometary activity. A plausible explanation for this color scatter is cometary activity, which is also assumed to explain the scatter of $B-V$ color indices reported by Sun et al. (2024). The heliocentric distance between consecutive observations with the o and c filters is always less than two hundredths of 1 au, which is insignificant to justify this color index scatter.

The increase in the $c-o$ color index scatter could make it difficult to identify a color trend in the comets, considering that the data were obtained at a lower sampling rate than that of the ATLAS network.

From the previous results of the analysis of the data of comets ATLAS and Palomar, it can be concluded that these comets show a heliocentric distance trend of the coma color. The comets ATLAS and Palomar tend to become bluer as they approach perihelion.

This color trend could be related to the physical properties of the comets, such as the different gas-to-dust ratio between the comets. The lack of a color trend could be due to a combination of a physical factor and/or observational bias due to the analysis of color samples with different sizes and ranges of variation in heliocentric distance.

4.5. Maximum Grain Size in the Coma During the Perihelion

The difference in the level of activity between the comets ATLAS and Palomar as suggested in Section 4.1 is probably related to their very different perihelion distances. One of the more obvious effects associated with these different levels of activity is the ability of the gas to lift dust particles from the surface of the nucleus. These dust grains ejected from the nucleus of comet ATLAS may have a larger diameter and consequently a larger mass than the corresponding grains on comet Palomar.

Parameters such as the minimum and maximum size of dust grains, their refractive index, and the exponent of a power-law size distribution can be used to describe the visible colors of a comet coma using the Mie light scattering theory (Kolokolova et al. 1997). It is clear that the calculation of the maximum dust size alone is not sufficient to explain the red and blue color of comets L3 and O3, as suggested in Section 4.4, but it is important to show the possible variability of this parameter with the perihelion distance.

The critical dust radius $a_{\rm crit}$ that can be lifted from a spherical nucleus was estimated using the equation from Meech & Svoren (2004), which is based on the drag force on a spherical grain

$$a_{\rm crit} = \frac{9\mu {\rm m_H} Q v_{\rm th}}{64\pi^2 \rho_{\rm g} \rho_{\rm n} R_{\rm n}^3 G}, \tag{8}$$

where μ is the atomic weight of the driving gas (amu), $\rm m_H$ is the mass of the hydrogen (kg), Q is the gas production rate (molecules $\rm s^{-1}$), $v_{\rm textth}$ is the mean thermal expansion speed of the gas, $\rho_{\rm g}$ and $\rho_{\rm n}$ are the grain and nuclear densities respectively, $R_{\rm n}$ is the nuclear radius and G is the gravitational constant.

Many of these parameters are difficult to define specifically for the comets ATLAS and Palomar, but due to the definition of their activity class in the Section 4.1, comets with almost similar physical properties can be used as a reference.

Assuming that the activity of comet ATLAS is determined by the volatilization of water at perihelion, its production rate Q was estimated using the relationship between Q (kg $\rm s^{-1}$) and the heliocentric distance r defined by the "Mark Kidger's and Observadores-cometas" group.[7]

$$Q = \frac{2.15 \times 10^4}{r^{1.55}}. \tag{9}$$

Considering $r = q = 3.55$ au, the water production of comet ATLAS is 1.01×10^{29} molecules $\rm s^{-1}$ less than the production of 4.28×10^{29} molecules $\rm s^{-1}$ of comet C/2014 Q2 (Lovejoy) at the time of perihelion using the pre-perihelion relationship defined by Combi et al. (2018). However, it is interesting to note that the perihelion distance of comet Lovejoy is 1.29 au, which is about one third of the perihelion distance of comet ATLAS.

[7] http://www.observadores-cometas.com/cometas/2019l3/qdust.html

The assumed outflow velocity of water is described by the equation given by Combi et al. (2004)

$$v_{\rm th} = \frac{0.85}{r^{0.5}}. \quad (10)$$

At $r = q = 3.55$ au, the gas velocity is 0.45 km s^{-1}.

The nuclear radius $R_{\rm N}$ was estimated using the equation defined by Betzler & de Sousa (2023)

$$\log_{10} R_N = 1.02 - 0.086 H_v. \quad (11)$$

where $H_{\rm v}$ ($=m(1,1)$) is the absolute magnitude determined from the visual apparent magnitudes provided by observers worldwide and available in the Comet Observation Database (COBS).[8]

The constants of Equation (11) were estimated from the visual COBS absolute magnitudes and mean radii of five nuclei of SPCs visited by space probes up to the publication of that manuscript by Betzler & de Sousa (2023). It is known that the absolute magnitude of SPCs is lower than that of LPCs, which could indicate a difference in the diameter of the two populations, which have a similar albedo. It is known that the absolute magnitude of SP comets is lower than that of LPCs, which could indicate a difference in the diameter of the two populations exhibiting similar albedo. In fact, Bauer et al. (2017) found that the SP comets of the Jupiter family had a mean nucleus size of 1.3 km in diameter in their debiased sample, while the mean size of the LP comets is about twice as large at 2.1 km. This suggests that LPCs have an effective radius greater than or equal to the radius defined by Equation (11). Using 752 visual COBS magnitudes, $H_{\rm v} = 1.5$, which leads to $R_{\rm N} = 7.9$ km, but it is easier to consider that $R_{\rm N} \geqslant 7.9$ km.

The structure of Equation (11) was originally proposed by Sosa & Fernández (2011) and assumes a cometary nucleus with the same bulk density $\rho_{\rm n}$ of 400 kg m^{-3} and similar activity level, independent of different gas/dust ratios.

The dust bulk density was assumed as 800 kg m^{-3} from Fulle et al. (2016).

Substituting the previous parameters into Equation (8), it is possible that the coma of comet ATLAS was populated with grains of size <1.9 mm at the time of perihelion.

The possible $a_{\rm crit}$ at perihelion of comet Palomar was certainly lower than the value calculated for comet ATLAS. Cometary activity is probably determined by the sublimation of super-volatile ices such as CO and CO_2.

The relationship between the CO rate Q and the heliocentric distance is not available in the literature for comet Palomar, but this rate was determined by Yang et al. (2021) for a comet with a typical activity level, C/2017 K2 (PANSTARRS) with $(1.6 \pm 0.5) \times 10^{27}$ molecules s^{-1} at 6.72 au. Due to the greater perihelion distance, the CO emission rate of comet Palomar at perihelion could therefore be $Q < 1.6 \times 10^{27}$ molecules s^{-1}.

[8] https://www.cobs.si/

The value of the gas expansion velocity was assumed to be <0.25 km s^{-1}, as suggested in the last cited reference.

The absolute magnitudes of comet Palomar are consistently brighter than those of comet ATLAS in the *o*- and *c*-filters. If the diameters of the nuclei are similar, the reason for a brighter absolute magnitude may be attributed to the differing active areas on the surface of the individual nuclei. If the nuclei maintain an approximately constant percentage of active area, such as approximately 10% observed in LPCs like C/1977 R1 (Kohler) (De Araújo et al. 2021) and C/1979 Y1 (Bradfield) (Sanzovo et al. 1996), then the nucleus of comet Palomar would be larger than that of comet ATLAS. Assuming this hypothesis to be correct, the radius of the nucleus of comet Palomar would be greater than 7.9 km.

Using the previously defined dust and nucleus density, the critical dust radius is <26 μm.

Typical cometary dust populations contain particles with a ratio of small (0.1–10) to large (10^3–10^5) μm size, which varies from comet to comet (Lisse et al. 2011). It is clear that the fraction between these two populations of dust grains ejected by comet Palomar overhangs to small particles at the time of perihelion.

4.6. Outliers and Candidates for Outbursts

Using Tukey's fence, seven outliers were found in the *G*-filter and 35 outliers in the *c*-filter data of comet ATLAS. The outliers in the *G*-filter data occurred before perihelion. In the *c*-band data, four outliers were identified after perihelion.

The seven outliers in the *G*-band data of comet ATLAS have a median apparent magnitude of 1.8 mag below the expected apparent magnitude calculated with Equation (1) using the parameters in Table 3. These outliers correspond to a heliocentric distance range of 8.2–5.4 au before perihelion. In this distance range there are 17 outliers or 49% of all outliers from the *c*-filter. These outliers identified from the *c*-filter are on median 0.5 mag less bright than the expected apparent magnitudes. This condition helps to reject the outburst hypothesis for these outliers.

Of the remaining 18 outliers in the *c*-filter, 14 measurements have brighter apparent magnitudes than those predicted by the model, and the last four outliers have an apparent magnitude 0.7 mag above those expected by the photometric model.

These 14 measurements can be divided into 10 events, some of which partially recorded the temporal evolution of the apparent brightness up to a local maximum and the subsequent decrease to a quiescent state, where the expected apparent magnitude is adjusted by Equation (1). The greatest peak brightness of these events had a magnitude amplitude of -7, which was determined by subtracting the expected and measured magnitudes. This magnitude amplitude is unusual when compared to the median value of -3 for outbursts on the centaur 29P/Schwassmann-Wachmann or -1 for outbursts on

Table 6
Candidates for Outbursts of the Comet Palomar. n is the Number of the Event in the Order in which they Occur, Defined by the Date of their Peak Values

n	Peak date (UT)	Δm
1	2021-09-13.279	-1.14 ± 0.02
2	2022-09-25.218	-0.98 ± 0.02

Note. Δm is the c-magnitude peak of the outburst in relation to the quiescence magnitude defined by Equation (1) with the corresponding parameters of Table 4.

SP and LPCs (Betzler et al. 2023; Betzler 2023). To investigate the nature of these events, an image with a field of view of 5 by 5′, provided by the Digital Sky Survey (DSS), was centered on the celestial coordinates of comet ATLAS for each corresponding observation time to investigate the presence of objects superimposed on the comet. Of the 10 events, stars in nine fields coincided with the position of the comet or were in its vicinity. The only probable real event is characterized by an increase in apparent magnitude of 0.34 mag compared to the expected magnitudes.

For comet Palomar there are 103 outliers in the o-filter and 33 outliers in the c-filter. Nine and 32 outliers in the c- and o-filter occurred after perihelion respectively. Of the 103 outliers in the o-filter, 61 events had a peak magnitude brighter than expected and correspond to outburst candidates. These candidates can be divided into 28 events, five of which occurred after perihelion. The largest peak brightness of these events had a magnitude amplitude close to −7, similar to that estimated for an event on comet ATLAS. Visual inspection of the DSS images shows that only two events before perihelion are likely to be outbursts (Table 6).

There are 16 candidates for outbursts in the c-filter, but all are false positives. These false positives were caused by the superposition of the comet with field stars.

An approximate estimate of the mass of the outbursts was calculated for each outburst in Table 6 using the method proposed by Ishiguro et al. (2016) and compared with similar events in other comets. To estimate this mass, the cross-section of the coma during each outburst was determined.

$$p_R C_c = 2.24 \times 10^{22} 10^{0.4(m_\odot - M(1,1,0))}. \quad (12)$$

The absolute magnitudes $M(1,1,0)$ of the peak values of outbursts 1 and 2 were calculated using Equation (2) and are 6.8 ± 0.4 and 7.2 ± 0.5 respectively. The coma cross-sections are 4.6×10^{10} and $3.2 \times 10^9\,\mathrm{m}^2$, respectively, for these outbursts.

These cross-sections correspond to a specific developmental phase of these events after their onset. In order to derive the cross-section caused by the outbursts, the coma cross-sections must be determined without their influence. A feasible way to achieve this is to use the expected absolute magnitudes of comet Palomar at each outburst to define the cross-sections and subtract them from the cross-sections caused by the outbursts. The expected magnitudes are 7.6 and 7.8, which imply an effective cross-section of 2.2×10^{10} and $1.9 \times 10^9\,\mathrm{m}^2$ for outbursts 1 and 2, respectively. The differences between the two corresponding cross-sections C_c were 2.5×10^{10} and $1.3 \times 10^9\,\mathrm{m}^2$.

The ejected mass during an outburst can be calculated with the equation

$$M_d = \frac{4}{3} \rho_d r_{\mathrm{eff}} C_c. \quad (13)$$

r_{eff} and ρ_d are the effective dust grain radius and mass density respectively. The radius r_{eff} is the typical size of dust grains and is responsible for the formation of the continuum.

The ejected mass M_d was calculated assuming a dust bulk density of $800\,\mathrm{kg\,m}^{-3}$ and $r_{\mathrm{eff}} = 14.2\,\mu$m. This last value was proposed by Wesołowski et al. (2020), who assumed that the cometary dust consists of a conglomerate of monomers with an average radius of 14.2 μm. This average size was estimated from the ratio between M_d and C_c of 45 outbursts observed by the Rosetta spacecraft on comet 67P/Churyumov-Gerasimenko (Lin et al. 2017) In particular, this particle size is reasonable considering the critical radius calculated in the previous section for this comet at perihelion.

The first event released 3.7×10^8 kg of dust, followed by event 2 with 1.9×10^8 kg. Considering the order of magnitude of the previously ejected masses, the fraction of the mass released by outburst 1 corresponds to 0.07% to 0.004% of the mass range of LPCs defined by Sosa & Fernández (2011). The masses M_d of outbursts 1 and 2 are compatible with the ejected mass of 15P/Finlay (Ishiguro et al. 2016), 29P/Schwassmann-Wachmann (Hosek et al. 2013), and 332P/Ikeya-Murakami (Ishiguro et al. 2014), but is two or three orders of magnitude smaller than the 2007 mega-outburst at 17P/Holmes (Li et al. 2011). Then the two events shown by comet Palomar can be described as "typical."

4.7. Photometric Profiles of the Comae

The photometric profiles of comets ATLAS and Palomar were derived by applying Equation (4) to the data sets obtained through filter G. There are 47 measurements of the slope s of the coma of comet ATLAS. This distribution is clearly asymmetric with a median $s = 1.2$ (Figure 9 top). The extreme value of the slope s of this distribution is 1.6 when this comet was at a heliocentric distance of 8.2 au.

The distribution of the slope s of comet Palomar comprises 34 measurements and can be fitted to a Gaussian distribution (Figure 9 bottom), as suggested by the Shapiro–Wilk test (p-value = 0.7498), and has a mean slope of 1.4 ± 0.2 (1σ).

Spearman's rank correlation coefficient is 0.64408, which indicates that a positive relationship between the slopes and the

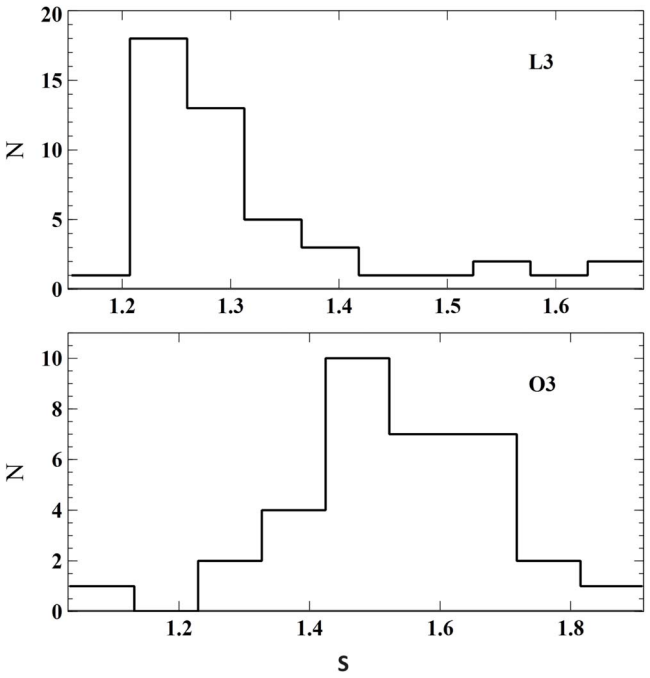

Figure 9. Histograms of the distribution of the photometric slopes s of the comae of comets ATLAS (L3) and Palomar (O3).

heliocentric distances for comet ATLAS can be considered statistically significant. In contrast, there is a non-significant small negative correlation between these two variables for comet Palomar ($rs = -0.2623$).

A classical interpretation for the values of the slopes of these two comets is the assumption that they indicate comets that are in a steady state in all or almost all of the observation periods considered. In particular, the slope m, which differs from unity but is in the range between 1 and 1.5, may be caused by the influence of the solar wind on the comets (Jewitt & Meech 1987). However, the influence of the solar wind is probably too weak to deform the comae of both comets in the heliocentric distance range, since the radiation force on a dust particle with the same cross-sectional area at 8 au from the Sun is only 1.5% above the value at 1 au (see Agarwal et al. 2023). Sun et al. (2024) have also reported slopes s greater than one and the stellar profiles during their observation window of comet ATLAS, between 2023 March and May. During this period, visual observers took 47 measurements of the degree of condensation (DC) of this comet's coma, which are available in the COBS database. DC is a measure of how condensed the coma is. More specifically, it provides a visual description of coma intensity over optocentric distance. It is measured on a scale from 0 to 9. The median value is 3, which means that the center of comet ATLAS' coma is much brighter than the edges, but still diffuse. Not surprisingly, the median value of the 10 DC estimates for comet Palomar obtained between 2022 August and 2024 January is 8, which means that the coma had an almost stellar aspect at its center, with a virtually invisible nebula around it.

Pilz (2017) argues that the DC scale is a direct consequence of a coma in free flow. In his simple but very interesting model, it is assumed that the same number N of gas and dust particles are present in each shell around the nucleus and that the density of gas and dust decreases with $1/\rho^2$. In a homogeneous coma, denoted by $\mathrm{DC} = 1$, each small volume contains the same amount of mass. This means that the integrated mass in each shell around the nucleus increases at the same rate as the surface area of these shells and that this increase is quadratic ($\Delta N/\Delta\rho \sim \rho^2$). A coherent approach for the last equation, when $\mathrm{DC} = 4.5$ for the free flow and $\mathrm{DC} = 1$ for the homogeneous coma, is $\Delta N/\Delta\rho \sim \rho^{\frac{4}{7}(\mathrm{DC}-1)}$.

It is clear that $\Delta N/\Delta\rho \sim \rho^{\frac{8}{7}}$ for comet ATLAS and $\Delta N/\Delta\rho \sim \rho^4$ for comet Palomar. It is obvious that the exponents of the previous equations derived from the median DC values for comet ATLAS and Palomar are different, with the value for the coma of the first comet being smaller. These exponents follow the same trend observed for the slopes s of these two comets.

Based on empirical measurements of the slope of comets ATLAS and Palomar and the earlier DC model, we can assume that the coma of these two comets was in a steady state during the observation period considered for the analysis. The slope $s > 1$ is most likely a direct consequence of their stellar appearance and not the influence of the solar radiation field due to their large heliocentric distance range ($3.6 \leqslant r \leqslant 10.2$ au), which was analyzed here.

5. Summary and Conclusions

This work analyzed the visible broadband data of the comets ATLAS and Palomar in the o- and c-filter of the ATLAS survey and in the G-band obtained at the Belgian Olmen observatory. The most important results of this work are presented below:

1. The dependence of the parameter Afρ measured with the G-filter on the photometric aperture radius ρ of the comets ATLAS and Palomar can be adjusted by a combination of Equations (3) and (4). From this fit it can be deduced that the Afρ parameter tends to a constant value for large ρ values (horizontal asymptote). This means that the use of large photometric apertures is recommended to allow comparison between photometric measurements of different observers. In this study, the maximum aperture $\rho = 42\farcs1$ was used to obtain all photometric parameters derived from the G-filter data.
2. The Af$\rho(0)(x_m = 0)$ at perihelion is $26{,}044 \pm 171$ cm for the comet ATLAS and 2069 ± 163 cm for the comet Palomar. According to the comet activity scheme proposed by Betzler et al. (2023), comet Palomar has a

typical activity level. Comet ATLAS is one of the unusual comets with high activity.

3. The absolute magnitudes $m(1,1)$ and the activity indices n in the o-filter for comet ATLAS are systematically brighter and larger than the values estimated with the c-filter, and both parameters are similar for comet Palomar.
4. The absolute magnitude in the G filter falls within the range of $m(1,1)$ magnitudes derived from the o and c filters for comet ATLAS, but consistently appears dimmer for both filters for comet Palomar. Additionally, the activity indices n show a systematic decrease for both comets. These variations in absolute magnitudes across filters are not attributed to dust color but rather to the duration of the observation campaign, which is significantly longer for ATLAS data compared to the Belgian data. A reduced observation period may capture phases of lower cometary activity occurring post-outburst or nucleus splitting events, contributing to the observed differences.
5. The cometary activity of comet ATLAS and Palomar probably began at $r > 13$ au and will end at $r > 14$ au, which means that the two comets could still be active until the second half of 2026. The activity of comets at these distances could be driven by the sublimation of low sublimation temperature materials such as carbon monoxide or dioxide and/or by exotic and rare cometary volatiles such as ammonia, formaldehyde or methane.
6. The absolute colors of comets ATLAS and Palomar are redder and bluer than the $c - o$ colors of the solar twin YBP 1194 respectively. The color $\Delta m(1,1)$ of comet Palomar is lower than the solar color despite its large error bar. The relative activity index Δn measures the gradient of the change in coma color with heliocentric distance. A negative relative index is associated with a blue coma color far from the Sun and a redder color at perihelion.
7. The critical dust radius that can be lifted from a spherical nucleus is less than 1.9 mm for comet ATLAS and less than 26 μm for comet Palomar, both at perihelion, which is related to the perihelion distance of these comets.
8. Tukey's fence outlier identification method was used to search for possible outliers in the ATLAS and Belgian data for comets ATLAS and Palomar. The outliers can be categorized by apparent magnitudes that are more or less bright than the expected magnitude given by Equation (1). The less bright events are likely to be moments when the comets show low activity. The brightest events are mostly false alarms where a bright field star has overlaid the comets. For the comet Palomar, only two candidates for an outburst could be identified in the c-filter data after perihelion.
9. The outburst candidates of comet Palomar had magnitude peaks of -1.14 ± 0.02 and -0.98 ± 0.02 in the c-band. Each event released an order of magnitude of 10^8 kg of dust, so these outbursts are classified as "typical" compared to similar phenomena on other comets.
10. The median slope s of the coma of comet ATLAS is 1.2. The mean slope s of comet Palomar is $1.4 \pm 0.2(1\sigma)$. These slopes indicate that the comas were in a steady state for the duration of the observation campaign of both comets. However, it is more likely that the slopes between 1 and 1.5 are associated with comas with bright inner parts and not only with the influence of the solar radiation field due their large heliocentric distance range ($3.6 \leqslant r \leqslant 10.2$ au) analyzed here.

Acknowledgments

This work has made use of data from the Asteroid Terrestrial-impact Last Alert System (ATLAS) project. The ATLAS project is primarily funded to search for near-earth asteroids through NASA grants NN12AR55G, 80NSSC18K0284, and 80NSSC18K1575; byproducts of the NEO search include images and catalogs from the survey area. This work was partially funded by Kepler/K2 grant J1944/80NSSC19K0112 and HST GO-15889, and STFC grants ST/T000198/1 and ST/S006109/1. The ATLAS science products have been made possible through the contributions of the University of Hawaii Institute for Astronomy, the Queen's University Belfast, the Space Telescope Science Institute, the South African Astronomical Observatory, and The Millennium Institute of Astrophysics (MAS), Chile.

The author thanks A. Diepvens of the Olmen Observatory (Belgium) for kindly making his invaluable data of the comets ATLAS and Palomar available on the Internet.

The author is grateful for the comet observations from the COBS Comet Observation Database provided by observers from around the world and used in this study.

The author thanks Orahcio Felicio de Sousa for his help in the initial stages of preparing this manuscript.

The author would like to thank an anonymous reviewer for his thorough and insightful feedback.

References

Agarwal, J., Kim, Y., Kelley, M. S. P., & Marschall, R. 2023, arXiv:2309.12759
A'Hearn, M. F., Feaga, L. M., Keller, H. U., et al. 2012, ApJ, 758, 29
A'Hearn, M. F., Millis, R. C., Schleicher, D. O., Osip, D. J., & Birch, P. V. 1995, Icar, 118, 223
A'Hearn, M. F., Schleicher, D. G., Millis, R. L., Feldman, P. D., & Thompson, D. T. 1984, AJ, 89, 579
Arakawa, S., & Wakita, S. 2024, PASJ, 76, 130
Ayala-Loera, C., Alvarez-Candal, A., Ortiz, J. L., et al. 2018, MNRAS, 481, 1848
Bauer, J. M., Grav, T., Fernández, Y. R., et al. 2017, AJ, 154, 53
Betzler, A. S. 2023, MNRAS, 523, 3678
Betzler, A. S. 2024, Ap&SS, 369, 10
Betzler, A. S., Almeida, R. S., Cerqueira, W. J., et al. 2017, AdSpR, 60, 612
Betzler, A. S., & de Sousa, O. F. 2020, NewA, 75, 101320
Betzler, A. S., & de Sousa, O. F. 2023, AN, 344, e20220084
Betzler, A. S., de Sousa, O. F., & Betzler, L. B. S. 2018, EM&P, 122, 53
Betzler, A. S., de Sousa, O. F., Diepvens, A., & Bettio, T. M. 2020, Ap&SS, 365, 102

Betzler, A. S., Diepvens, A., & de Sousa, O. F. 2023, MNRAS, 526, 246
Biver, N., Bockelée-Morvan, D., Debout, V., et al. 2014, A&A, 566, L5
Blaauw, R. C., Suggs, R. M., & Cooke, W. J. 2014, M&PS, 49, 45
Combi, M. R., Harris, W. M., & Smyth, W. H. 2004, in Comets II, ed. M. C. Festou, H. U. Keller, & H. A. Weaver (Tucson, AZ: Univ. Arizona Press), 523
Combi, M. R., Mäkinen, T. T., Bertaux, J. L., Quémerais, E., Ferron, S., et al. 2018, Icar, 300, 33
Dahiru, T. 2008, Annals of Ibadan Postgraduate Medicine, 6, 21
De Araújo, L., Boice, D., Sanzovo, G. C., & De Almeida, A. A. 2021, in 43rd COSPAR Scientific Assembly, 309
Delsemme, A. H. 1982, in IAU Colloq. 61: Comets (Tucson, AZ: Univ. Arizona Press), 85
Ehlert, S., Moticska, N., & Egal, A. 2019, AJ, 158, 7
Eistrup, C., Walsh, C., & van Dishoeck, E. F. 2019, A&A, 629, A84
Faggi, S., Mumma, M. J., Villanueva, G. L., Paganini, L., & Lippi, M. 2019, AJ, 158, 254
Ferrín, I. 2010, P&SS, 58, 365
Filacchione, G., Capaccioni, F., Ciarniello, M., et al. 2020, Natur, 578, 49
Fulle, M., Marzari, F., Della Corte, V., et al. 2016, ApJ, 821, 19
Hadraoui, K., Cottin, H., Ivanovski, S. L., et al. 2019, A&A, 630, A32
Harrington Pinto, O., Womack, M., Fernandez, Y., & Bauer, J. 2022, PSJ, 3, 247
Henden, A. A. 2019, JAVSO, 47, 130
Holmberg, J., Flynn, C., & Portinari, L. 2006, MNRAS, 367, 449
Hosek, M. W., Blaauw, J., Cooke, R. C., & Suggs, W. J. 2013, AJ, 145, 122
Howell, S. B. 2000, Handbook of CCD Astronomy (Cambridge: Cambridge Univ. Press)
Hughes, D. W. 1989, A&A, 220, 301
Ishiguro, M., Jewitt, D., Hanayama, H., et al. 2014, ApJ, 787, 55
Ishiguro, M., Kuroda, D., Hanayama, H., et al. 2016, AJ, 152, 169
Jehin, E., Moulane, Y., Manfroid, J., et al. 2022, ATel, 15186, 1
Jewitt, D. 2015, AJ, 150, 201
Jewitt, D., Hui, M.-T., Mutchler, M., et al. 2017, ApJL, 847, L19
Jewitt, D., & Meech, K. J. 1988, AJ, 96, 1723
Jewitt, D. C., & Meech, K. J. 1987, ApJ, 317, 992
Kaib, N. A. 2022, SciA, 8, eabm9130
Kelley, M. S. P., Kokotanekova, R., Holt, C. E., et al. 2022, ApJL, 933, L44
Knight, M. M., Kokotanekova, R., & Samarasinha, N. H. 2023, arXiv:2304.09309
Kolokolova, L., Jockers, K., Chernova, G., & Kiselev, N. 1997, Icar, 126, 351
Krankowsky, D. 1991, in IAU Colloq. 116: Comets in the Post-Halley Era, ed. R. L. Newburn, Jr., M. Neugebauer, & J. Rahe (Dordrecht: Kluwer), 855
Królikowska, M., & Dybczyński, P. A. 2017, MNRAS, 472, 4634
Le Feuvre, M., & Wieczorek, M. A. 2008, Icar, 197, 291
Leibowitz, E. M., & Brosch, N. 1986a, Icar, 68, 430
Leibowitz, E. M., & Brosch, N. 1986b, Icar, 68, 418
Li, J., Jewitt, D., Clover, J. M., & Jackson, B. V. 2011, ApJ, 728, 31
Lin, Z.-Y., Knollenberg, J., Vincent, J. B., et al. 2017, MNRAS, 469, S731
Lisse, C. M., Kissel, J., Melosh, H. J., et al. 2011, in EPSC-DPS Joint Meeting 2011, 870
Liu, F., Asplund, M., Yong, D., et al. 2016, MNRAS, 463, 696
Marsden, B. G., & Sekanina, Z. 1973, AJ, 78, 1118
Mazzotta Epifani, E., Dall'Ora, M., di Fabrizio, L., et al. 2010, A&A, 513, A33
Meech, K. J., & Svoren, J. 2004, in Comets II, ed. M. C. Festou, H. U. Keller, & H. A. Weaver (Tucson, AZ: Univ. Arizona Press), 317
Moro, D., & Munari, U. 2000, A&AS, 147, 361
Moulane, Y., Jehin, E., Manfroid, J., et al. 2023, A&A, 670, A159
Natenzon, M. Y., Neishtadt, A. I., Sagdeev, R. Z., Seryakov, G. K., & Zaslavsky, G. M. 1990, PhLA, 145, 255
Picazzio, E., Luk'yanyk, I. V., Ivanova, O. V., et al. 2019, Icar, 319, 58
Pilz, U. 2017, Der kondensationsgrad von kometen comets: the degree of condensation, a new approach.
Sanzovo, G. C., Singh, P. D., & Huebner, W. F. 1996, A&AS, 120, 301
Shi, J., Xu, R., Ma, Y., et al. 2023, ApJ, 943, 26
Smith, K. W., Smartt, S. J., Young, D. R., et al. 2020, PASP, 132, 085002
Solontoi, M., Ivezić, Z. ˇ, Jurić, M., et al. 2012, Icar, 218, 571
Sosa, A., & Fernández, J. A. 2011, MNRAS, 416, 767
Stebbins, J., & Kron, G. E. 1957, ApJ, 126, 266
Sun, S., Shi, J., Ma, Y., & Zhao, H. 2024, MNRAS, 529, 1617
Tonry, J. L., Denneau, L., Heinze, A. N., et al. 2018, PASP, 130, 064505
Tukey, J. W. 1977, Exploratory Data Analysis (Addison-Wesley: Reading, MA)
Vanysek, V. 1983, in Asteroids, Comets, and Meteors (Uppsala: Astronomiska Observatoriet), 355
Weissman, P. R. 1996, in ASP Conf. Ser. 107, Completing the Inventory of the Solar System, ed. T. Rettig & J. M. Hahn (San Francisco, CA: ASP), 265
Wesołowski, M., Gronkowski, P., & Tralle, I. 2020, P&SS, 184, 104867
Wiegert, P., & Tremaine, S. 1999, Icar, 137, 84
Willacy, K., Turner, N., Bonev, B., Gibb, E., Dello Russo, N., et al. 2022, ApJ, 931, 164
Willmer, C. N. A. 2018, ApJS, 236, 47
Womack, M., Sarid, G., & Wierzchos, K. 2017, PASP, 129, 031001
Yabushita, S. 1989, MNRAS, 240, 69
Yang, B., Jewitt, D., Zhao, Y., et al. 2021, ApJL, 914, L17
Zhilyaev, B. E., Vid'machenko, A., Petukhov, V. N., et al. 2021, AstSR, 17, 1
Zimbelman, J. R. 1984, Icar, 57, 48